Effect of Initial Monomer Concentration on Spatial Inhomogeneity in Poly(acrylamide) Gels

ARTICLE *in* MACROMOLECULES · AUGUST 2003

Impact Factor: 5.8 · DOI: 10.1021/ma021366u

2 AUTHORS, INCLUDING:

Oguz Okay
Istanbul Technical University
154 PUBLICATIONS **4,131** CITATIONS

SEE PROFILE

Effect of Initial Monomer Concentration on Spatial Inhomogeneity in Poly(acrylamide) Gels

Mine Yener Kizilay and Oguz Okay*

Department of Chemistry, Istanbul Technical University, 80626 Maslak, Istanbul, Turkey

Received August 21, 2002; Revised Manuscript Received December 2, 2002

ABSTRACT: The spatial inhomogeneity in poly(acrylamide) (PAAm) gels has been investigated with the static light scattering technique. Three different sets of PAAm gels were prepared, each at a fixed chemical cross-link density but at various initial monomer concentrations. The gels were characterized by swelling and elasticity tests as well as by light scattering measurements at a gel state just after their preparation. A critical polymer network concentration was found where the degree of the inhomogeneity in PAAm gels attains a maximum value. This phenomenon was explained as a result of two opposite effects of the initial monomer concentration on the gel inhomogeneity. Increasing monomer concentration increases both the effective cross-link density and the polymer concentration of the hydrogels. While the inhomogeneity becomes larger due to the first effect, the latter effect decreases the apparent gel inhomogeneity. The interplay of these two opposite effects determines the spatial inhomogeneity in PAAm gels. The theory proposed by Panyukov and Rabin also predicts the appearance of a maximum degree of spatial gel inhomogeneity at a critical polymer network concentration.

Introduction

Hydrogels are important materials of both fundamental and technological interest. They are usually prepared by free-radical cross-linking copolymerization of a monovinyl monomer with a divinyl monomer (cross-linker) in a homogeneous solution. Swelling properties and the elastic behavior of hydrogels have been intensively studied in the past four decades. However, theories are still unable to predict their physical properties from the synthesis conditions. This is due to the several nonidealities of the gel formation system such as the different and conversion-dependent reactivities of the vinyl groups, cyclization, multiple cross-linking, and diffusion-controlled reactions.[1,2] Hydrogels formed in such a nonideal picture necessarily include defects affecting their physical properties such as swelling, elasticity, transparency, and permeability.

One of the network defects, which have been extensively studied, is the gel inhomogeneity.[3,4] In contrast to the ideal gels with a homogeneous distribution of cross-links throughout the gel sample, real gels always exhibit an inhomogeneous cross-link density distribution, known as the spatial gel inhomogeneity. Since the gel inhomogeneity is closely connected to the spatial concentration fluctuations, scattering methods such as light scattering,[5,6] small-angle X-ray scattering,[5,7] and small-angle neutron scattering[8−10] have been employed to investigate the spatial inhomogeneities. The gel inhomogeneity can be manifested by comparing the scattering intensities from the gel and from a semidilute solution of the same polymer at the same concentration. The scattering intensity from gels is always larger than that from the polymer solution. The excess scattering over the scattering from polymer solution is related to the degree of the inhomogeneities in gels.

The spatial inhomogeneity in acrylamide (AAm)-based hydrogels has been investigated as a function of a number of parameters, such as the cross-link density,[11−14] the type of the cross-linker,[15] the ionization degree,[3,4,16] the swelling ratio,[4,17] and the temperature.[18] In general, the gel inhomogeneity increases significantly with the cross-link density. A reduced reactivity of the cross-linker used in the hydrogel preparation also leads to a higher degree of inhomogeneity. On the other hand, the inhomogeneity decreases with the ionization degree of gels. An enhancement of the excess scattering is generally observed, if the gel swells beyond its swelling degree after preparation.

The polymer network concentration at the state of gel preparation alters the gel structure and, in turn, alters the gel properties.[19] Decreasing the polymer concentration prior to cross-linking causes the polymer chains to disentangle, so that the network formed in a dilute solution can swell highly when exposed to a good solvent. On the other hand, decreasing polymer concentration increases the probability of cyclization and multiple cross-linking reactions during the gel formation process, so that a large fraction of cross-linker molecules are wasted in ineffective cross-links.[20] The effect of the polymer network concentration at the state of gel preparation on the gel inhomogeneity has not been reported before. In the present work, we prepared three sets of poly(acrylamide) (PAAm) gels at various initial monomer concentrations. The cross-linker ratio X, which is the mole ratio of the cross-linker N,N'-methylenebis(acrylamide) (BAAm) to the monomer AAm, was fixed at 1/61.5, 1/66, and 1/100 in each set of gels. The gels were characterized by swelling and elasticity tests as well as by static light scattering measurements at a gel state just after their preparation. An equivalent semidilute PAAm solution served as a reference in the understanding of the inhomogeneities in gels. The excess scattering from the gels is taken as a measure of their inhomogeneity.

Experimental Section

Synthesis of Hydrogels. Acrylamide (AAm, Merck), N,N'-methylenebis(acrylamide) (BAAm, Merck), ammonium persulfate (APS, Merck), and N,N,N',N'-tetramethylethylenedi-

* Corresponding author.

10.1021/ma021366u CCC: $25.00
Published on Web 08/08/2003

amine (TEMED) were used as received. PAAm gels were prepared by free-radical cross-linking copolymerization of AAm and BAAm in an aqueous solution at 24 °C in the presence of 2.63 mM APS initiator and 0.375% v/v TEMED accelerator. The gels were prepared as three sets; in each set, the initial molar concentration of the monomers, denoted by C_0, was varied between 0.36 and 2.09 M while the cross-linker ratio X (the mole ratio of BAAm to AAm) was fixed at 1/61.5, 1/66, or 1/100. The reaction time was 1 day. Details about the gel synthesis have been reported elsewhere.[21]

PAAm Network Concentration at the Stage of Gel Preparation. The degree of dilution of the networks after their preparation was denoted by ν_2^0, the volume fraction of cross-linked polymer after the gel preparation. To determine ν_2^0, PAAm hydrogels after preparation were first swollen in water over a period of at least one month until no further extractable polymer could be detected. The hydrogels after extraction were first deswollen in water−acetone mixtures and then dried at 90 °C under vacuum to constant weight. Details about the extraction procedure were described previously.[22] Assuming that the monomer conversions were complete after the cross-linking copolymerization, the theoretical value of ν_2^0 can also be calculated from the initial molar concentration of the monomers C_0 as $\nu_2^0 = 10^{-3}C_0V_r$, where V_r is the molar volume of PAAm repeat units (52.6 mL/mol). Measurements showed that the experimental value of ν_2^0 is close to its theoretical value in the range of ν_2^0 between 0.02 and 0.11, indicating that, under the reaction conditions, the monomer conversions and the gel fractions are complete.

Swelling Measurements in Water. The hydrogels in the form of rods of 4 mm in diameter were cut into samples of about 10 mm length. Then, each sample was placed in an excess of water at 24 ± 0.5 °C. To reach swelling equilibrium, the hydrogels were immersed in water for at least 2 weeks, replacing the water every other day. The swelling equilibrium was tested by measuring the diameter of the gel samples. To achieve good precision, three measurements were carried out on samples of different length taken from the same gel. The normalized volume of the equilibrium swollen hydrogels V_{eq} (volume of equilibrium swollen gel/volume of the gel just after preparation) was determined by measuring the diameter of the hydrogel samples by a calibrated digital compass (Mitutoyo Digimatic Caliper, Series 500, resolution 0.01 mm). V_{eq} was calculated as $V_{eq} = (D/D_0)^3$, where D and D_0 are the diameter of hydrogels after equilibrium swelling in water and after synthesis, respectively. The volume fraction of cross-linked polymer in the equilibrium swollen gel $\nu_{2,eq}$was calculated as $\nu_{2,eq} = \nu_2^0/V_{eq}$.

Mechanical Measurements. Uniaxial compression measurements were performed on gels just after their preparation. All the mechanical measurements were conducted in a thermostated room of 24 ± 0.5 °C. The stress−strain isotherms were measured by using an apparatus previously described.[23] Briefly, a cylindrical gel sample of about 6 mm in diameter and 7 mm in length was placed on a digital balance (Sartorius BP221S; readability and reproducibility: 0.1 mg). A load was transmitted vertically to the gel through a road fitted with a PTFE end-plate. The compressional force acting on the gel was calculated from the reading of the balance. The resulting deformation was measured after 20 s of relaxation by using a digital comparator (IDC type Digimatic Indicator 543-262, Mitutoyo Co.), which was sensitive to displacements of 10^{-3} mm. The measurements were conducted up to about 15% compression. Reversibility of the isotherms was tested by recording the force and the resulting deformation during both force-increasing and force-decreasing processes. The two processes yielded almost identical stress−strain relations. From the repeated measurements, the standard deviations in the modulus value were less than 3%. The sample weight loss during the measurements due to water evaporation was found to be negligible. The elastic modulus G_0 was determined from the slope of linear dependence $f = G_0(\alpha - \alpha^{-2})$, where f is the force acting per unit cross-sectional area of the undeformed gel specimen and α is the deformation ratio (deformed length/initial length). For a network of Gaussian chains, the elastic modulus at the state of gel preparation G_0 is related to the effective cross-link density ν_e by[24,25]

$$G_0 = A\nu_e RT\nu_2^0 \tag{1}$$

where the front factor A equals to 1 for an affine network and $1 - 2/\phi$ for a phantom network, where ϕ is the functionality of the cross-links; R and T have their usual meanings. The number of segments between two successive cross-links N is related to the cross-link density by

$$N = 1/(\nu_e V_1) \tag{2}$$

where V_1 is the molar volume of a segment, which is taken as the molar volume of water (18×10^{-6} m^3/mol).

Light Scattering Experiments. For the light scattering measurements, the cross-linking polymerizations were carried out in the light scattering vials. All glassware was kept dust-free by rinsing in hot acetone prior using. The solutions were filtered through membrane filters (pore size = 0.2 μm) directly into the vials. This process was carried out in a dust-free glovebox. All the gels subjected to light scattering measurements were clear and appeared homogeneous to the eye. For the calculation of excess scattering from gels, all the cross-linking polymerizations were repeated under the same experimental conditions, except that the cross-linker BAAm was not used.

The light scattering measurements were carried out at 24 °C using a commercial multiangle light scattering DAWN EOS (Wyatt Technologies Corp.) equipped with a vertically polarized 30 mW gallium arsenide laser operating at $\lambda = 690$ nm and 18 simultaneously detected scattering angles. The scattered light intensities were recorded from 51.5° to 142.5° which correspond to the scattering vector q range 1.1×10^{-3}−2.3×10^{-3} Å^{-1}, where $q = (4\pi n/\lambda)\sin(\theta/2)$, θ is the scattering angle, λ is the wavelength of the incident light in a vacuum, and n is the refractive index of the medium. The light scattering system was calibrated against a toluene standard. To obtain the ensemble-averaged light scattering intensity of gels, eight cycles of measurements with a small rotation of the vial between each cycle were averaged.

Results and Discussion

The results from swelling and elasticity tests are plotted in Figure 1. The filled and open circles represent the results of measurements for gel samples with the cross-linker ratio $X = 1/61.5$ and 1/66, respectively, and the filled triangles for samples with $X = 1/100$. In Figure 1A, the volume fraction of cross-linked polymer in the equilibrium swollen gel $\nu_{2,eq}$ and the elastic modulus of gels after preparation G_0 are shown as a function of ν_2^0. From the modulus data and assuming phantom network behavior ($\phi = 4$), the effective cross-link densities ν_e of the hydrogels were calculated using eq 1. The results are shown in Figure 1B. Figure 1C shows ν_2^0 dependence of the cross-linking efficiency of BAAm ϵ_{xl}, that is, the fraction of BAAm forming effective cross-links. ϵ_{xl} was calculated using the equation $\epsilon_{xl} = \nu_e/\nu_{chem}$, where ν_{chem} is the chemical cross-link density, which would result if all BAAm molecules formed effective cross-links in the hydrogel. The lines in the figures are best fits to the data, and they were drawn for the eye.

As expected, both $\nu_{2,eq}$ and ν_e are increasing functions of ν_2^0. Thus, increasing the polymer network concentration at the gel preparation (ν_2^0) results in decreased swelling ratios and increased effective cross-link densities of the hydrogels. This is a consequence of the decrease of probability of cyclization and multiple cross-linking reactions as the initial monomer concentration

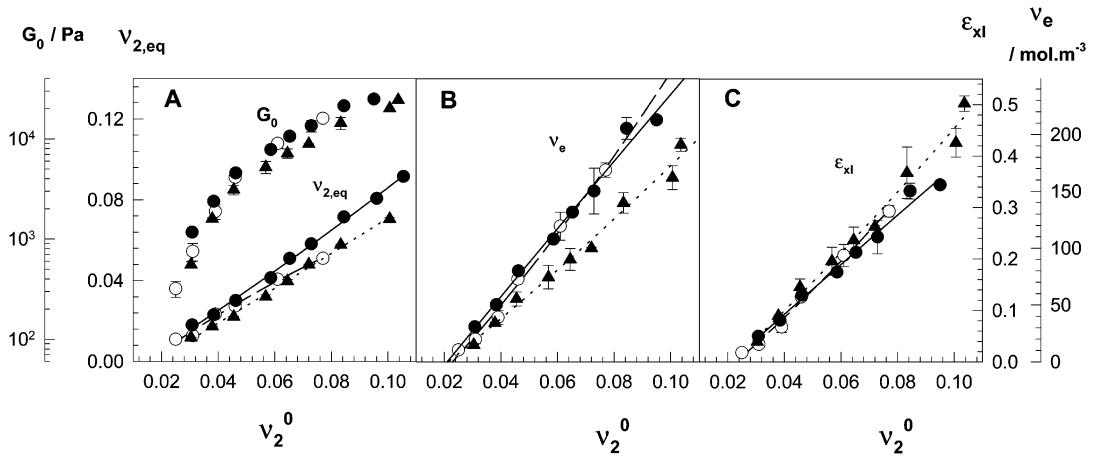

Figure 1. **(**A**)** Volume fraction of cross-linked polymer in the equilibrium swollen gel $\nu_{2,eq}$ and the elastic modulus of gels after preparation G_0 shown as a function of ν_2^0. **(**B**)** Effective cross-link density ν_e of the hydrogels shown as a function of ν_2^0. **(**C**)** Cross-linking efficiency of BAAm ϵ_{xl} shown as a function of ν_2^0. The cross-linker ratio X of the hydrogels: 1/61.5 (●), 1/66 (○), and 1/100 (▲). Temperature = 24 °C. The lines are best fits to the data, and they were drawn for the eye.

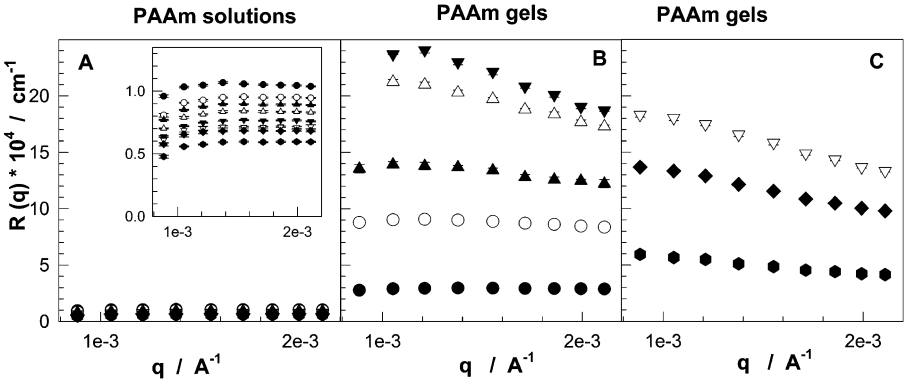

Figure 2. Rayleigh ratio $R(q)$ vs scattering vector q plots for the PAAm gels (B and C) and for the corresponding linear PAAm solutions (A). X = 1/61.5, ν_2^0 = 0.019 (●), 0.030 (○), 0.039 (▲), 0.046 (△), 0.058 (▼), 0.065 (▽), 0.073 (◆), and 0.096 (⬢).

increases. Indeed, the cross-linking efficiency ϵ_{xl} rapidly increases with ν_2^0 from 0.02 to 0.5. Figure 1B also shows that the best-fit line through the ν_e vs ν_2^0 data does not intersect with the origin, but intersects with the positive abscissa. This result is similar to that reported by Baker et al.[19] This also illustrates the importance of cyclization and multiple cross-linking reactions during the formation of PAAm gels. The effect of the cross-linker content on the properties of gels is also apparent from the comparison of the results of three sets of gels. Both ν_e and $\nu_{2,eq}$ increase while ϵ_{xl} decreases as the cross-linker ratio X is increased. This is due to the fact that increasing cross-linker concentration increases the probability of cross-linking and cyclization reactions during the gel formation process.[1] While the effective cross-link density ν_e of gels increases due to the first effect, the latter effect decreases the efficiency of cross-linking.

Light scattering measurements were carried out on hydrogels prepared in the range of ν_2^0 between 0.019 and 0.11. Figure 2 shows the Rayleigh ratio $R(q)$ vs the scattering vector q plots for PAAm hydrogels prepared at X = 1/61.5 and for the corresponding linear PAAm solutions. Compared to gels, the light scattering intensity from polymer solutions does not change much both with the scattering vector q and with the polymer concentration ν_2^0 (Figure 2A). However, a closer examination of the solution data shown as inset to Figure 2A indicates a slight decrease of the scattered light intensity from polymer solution with increasing concentration. Figure 2B,C shows that the scattering light intensity from gels first increases with increasing polymer concentration up to a critical value but then decreases again. Similar results were also obtained using gel samples prepared at X = 1/66 and 1/100. Thus, the results clearly show the existence of two gel regimes having opposite ν_2^0 dependence. Another point shown in Figure 2 is that $R(q)$ becomes increasingly q dependent as ν_2^0 is increased.

Excess scattering intensities $R_{ex}(q)$ were calculated as $R_{ex}(q) = R_{gel}(q) - R_{sol}(q)$, where $R_{gel}(q)$ and $R_{sol}(q)$ are the Rayleigh ratios for gel and polymer solution, respectively. To compare the excess scattering of different gels, we will focus on the scattering intensity measured at a fixed scattering vector $q = 1 \times 10^{-3}$ Å^{-1}. Figure 3 shows $R_{gel,q}$ (filled circles), $R_{sol,q}$ (open circles), and the excess scattering $R_{ex,q}$ (filled triangles) at $q = 1 \times 10^{-3}$ Å^{-1} plotted as a function of ν_2^0 for three sets of gels. In polymer solutions, the scattered light intensity $R_{sol,q}$ decreases only slightly with ν_2^0. However, $R_{gel,q}$ and $R_{ex,q}$ increase rapidly with ν_2^0 and, after passing a maximum at a critical polymer concentration ($\nu_{2,cr}^0$), decrease again. Figure 3 also shows that the maximum becomes more dominant as the cross-linker ratio X is increased. Since $R_{ex}(q)$ is a measure of the spatial inhomogeneity in a gel, the results indicate that the PAAm gels formed at $\nu_{2,cr}^0$ exhibit the highest degree of

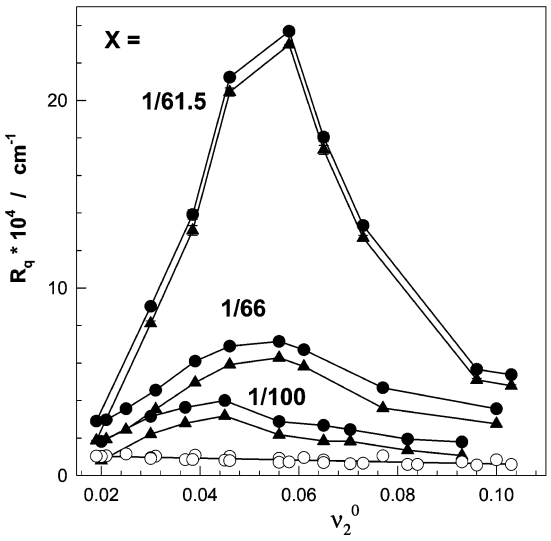

Figure 3. Scattering light intensities from gels $R_{gel,q}$ (●), from PAAm solutions $R_{sol,q}$ (○), and the excess scattering $R_{ex,q}$ (▲) measured at $q = 1 \times 10^{-3}$ Å^{-1} shown as a function of ν_2^0. The cross-linker ratios X used in the gel preparation are indicated in the figure.

inhomogeneity. While for $\nu_2^0 < \nu_{2,cr}^0$ the gel becomes more inhomogeneous with increasing polymer concentration, for $\nu_2^0 > \nu_{2,cr}^0$ the inhomogeneity decreases with the polymer concentration. The critical polymer concentration $\nu_{2,cr}^0$ was found to be 0.062 ± 0.004, 0.054 ± 0.007, and 0.051 ± 0.005 for the cross-linker ratio X = 1/61.5, 1/66, and 1/100, respectively, indicating that $\nu_{2,cr}^0$ slightly shifts toward higher polymer concentrations as the cross-link density increases.

To interpret light scattering results from gels, several functional forms of excess scattering $R_{ex}(q)$ have been proposed empirically, i.e., Debye−Bueche,[26−29] Guinier,[30−33] and Ornstein−Zernicke functions.[30−34] For example, the excess scattering was given by the Debye−Bueche function as

$$R_{ex}(q) = \frac{4\pi K\xi^3\langle\eta^2\rangle}{(1 + q^2\xi^2)^2} \tag{3}$$

where K is the optical constant, $K = 8\pi^2 n^2 \lambda^{-4}$, ξ is the correlation length of the scatterers, and $\langle\eta^2\rangle$ is the mean-square fluctuation of the refractive index. According to eq 3, the slope and the intercept of $R_{ex}(q)^{-1/2}$ vs q^2 plot (Debye−Bueche plot) give ξ and $\langle\eta^2\rangle$ of a gel sample. In Figure 4, the excess scattering data from gel samples prepared at X = 1/66 are given in the form of Debye−Bueche plots. It is seen that straight lines are obtained in this analysis, indicating that the Debye−Bueche function works well. Such straight lines were also obtained for other sets of gels prepared at X = 1/61.5 and 1/100. In fact, ln $R_{ex}(q)$ vs q^2 and $R_{ex}(q)^{-1}$ vs q^2 plots also give straight lines, implying that the Guinier and Ornstein−Zernicke functions also work well. Calculated values of ξ and $\langle\eta^2\rangle$ from the Debye−Bueche analysis are shown in Figure 5 plotted as a function of ν_2^0. The correlation length of the scatterers ξ and the mean-square fluctuations $\langle\eta^2\rangle$ are in the range 6−27 nm and 10^{-7}−10^{-6}, respectively. ξ decreases while $\langle\eta^2\rangle$ increases as the polymer concentration ν_2^0 decreases up to about 0.04. Between ν_2^0 = 0.02 and 0.04, $\langle\eta^2\rangle$ exhibits a maximum for each set of gels. Thus, the Debye−Bueche method also shows a maximum degree of inhomogeneity in PAAm gels formed at a critical value of ν_2^0, but the maximum is shifted toward a lower range of polymer concentrations. Similar results were also obtained by fitting the data to the Guinier and Ornstein−Zernicke functions.

The approaches mentioned above, however, assume the functional form of $R_{ex}(q)$ on q without detailed discussion about its validity. Recently, Panyukov and Rabin proposed a statistical theory for describing the structure factor for gels.[35] The Panyukov−Rabin (PR) theory assumes that the gel is prepared by instantaneous cross-linking of semidilute polymer solutions. The theory also assumes that the gel formed is sufficiently far away from the gel point, and the permanent entanglements do not contribute to the rubber elasticity of gel. Despite these limitations to the applicability of the PR theory, it succeeded in predicting qualitatively the cross-link and charge density dependences of the spatial inhomogeneity in gels formed by free-radical cross-linking mechanism.[12,13] Therefore, we employed this theory in order to elucidate the effect of initial monomer concentration on the spatial inhomogeneity in PAAm gels.

The PR theory takes into account the effect of the network structure at preparation on the structure factor $S(q)$ under condition of measurements. The structure factor of this theory also consists of two contributions, one from the thermal fluctuations $G(q)$ and the other from the static inhomogeneities $C(q)$. Theoretical prediction of the PR theory requires the network parameters at the state of the gel preparation as well as at the state of the measurements. The final equations of this theory are

$$S(q) = G(q) + C(q) \tag{4}$$

$$G(q) = \frac{a^{-3}\nu_2 N g(q)}{1 + w g(q)} \tag{5}$$

$$C(q) = \frac{a^{-3}\nu_2 N}{(1 + w g(q))^2 (1 + Q^2)^2} \times \left(6 + \frac{9}{w_0 - 1 + 0.5Q^2(\nu_2^0/\nu_2)^{2/3}(\nu_2^0)^{-1/4}}\right) \tag{6}$$

where a is the segment length, ν_2 is the volume fraction of cross-linked polymer in the gel at the measurement, which is equal to ν_2^0 for the measurement just after gel preparation, and $g(q)$ is the thermal correlator in the absence of the excluded-volume effect,

$$g(q) = \frac{1}{0.5Q^2 + (4Q^2)^{-1} + 1} + \frac{2(\nu_2/\nu_2^0)^{2/3}(\nu_2^0)^{1/4}}{(1 + Q^2)^2} \tag{7}$$

w and w_0 are the excluded-volume parameters at the state of measurement and at gel preparation, respectively:

$$w = (1 - 2\chi + \nu_2)\nu_2 N \tag{8}$$

$$w_0 = (\nu_2^0)^{5/4} N \tag{9}$$

Q is the reduced scattering vector normalized by the monomer fluctuating radius, $Q = aN^{1/2}q$, χ is the polymer−solvent interaction parameter, and the initial

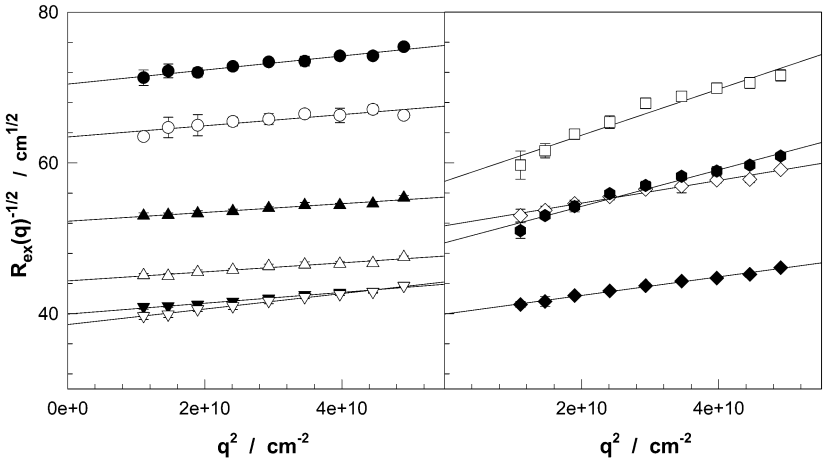

Figure 4. Debye−Bueche plots for PAAm gels prepared at $X = 1/66$. $\nu_2^0 = 0.021$ (●), 0.025 (○), 0.031 (▲), 0.039 (△), 0.046 (▼), 0.056 (▽), 0.061 (◆), 0.077 (◇), 0.087 (⬢), and 0.100 (□).

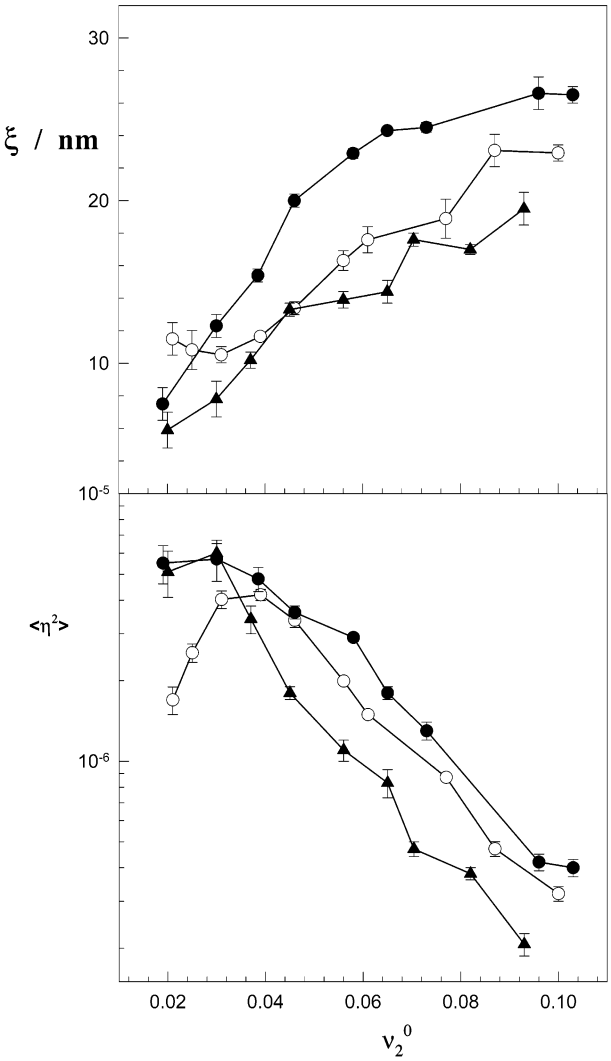

Figure 5. Correlation length of the scatterers ξ and the mean-square fluctuation of the refractive index $\langle\eta^2\rangle$ in PAAm gels shown as a function of ν_2^0. The cross-linker ratio X of the hydrogels: 1/61.5 (●), 1/66 (○), and 1/100 (▲).

state of the gels is assumed to be in a good solvent (the scaling) regime while the final state is taken as a poor solvent (mean field) regime. Note that N relates to ν_e through eq 2, and it is inversely proportional to the effective cross-link density.

Since we already know the PAAm network parameters N and ν_2^0 from the swelling and elasticity measurements of gels, PR theory can be used for the present system as a parameter-free theory. Nonlinear curve fit to the experimental ν_e vs ν_2^0 data shown in Figure 1B for each set of gels gives the following relations

$$\nu_e\,(\text{mol m}^{-3}) = (NV_1)^{-1} = -64 + 3064\nu_2^0 - 691(\nu_2^0)^2 \quad (X = 1/61.5) \quad (10a)$$

$$= -61 + 2509\nu_2^0 + 6453(\nu_2^0)^2 \quad (X = 1/66) \quad (10b)$$

$$= -42 + 1888\nu_2^0 + 2540(\nu_2^0)^2 \quad (X = 1/100) \quad (10c)$$

which were solved for N, the number of segments between two successive cross-links, as a function of ν_2^0. Moreover, using the equilibrium swelling ratios and the effective cross-link densities of the hydrogels, the interaction parameter χ between the PAAm network and water may be obtained by solving the Flory−Rehner equation

$$\ln(1 - \nu_{2,eq}) + \nu_{2,eq} + \chi\nu_{2,eq}^2 + 0.5\nu_e V_1 \nu_{2,eq}^{1/3}(\nu_2^0)^{2/3} = 0 \quad (11)$$

for χ as a function of $\nu_{2,eq}$. By least squares, we obtained

$$\chi = 0.481 \pm 0.005 \quad (12)$$

in the range of $\nu_{2,eq}$ between 0.011 and 0.070. This value of the χ parameter of the PAAm−water system is in good agreement with the reported value of 0.48,[19,36] and it is independent of ν_2 in the range of interest.

Using eqs 4−10 and assuming that the segment length equals 8 Å, the structure factor $S(q)$, its thermal fluctuations correlator $G(q)$, and the part of static density inhomogeneities $C(q)$ were calculated. Calculations were for the scattering vector $q = 0.001$ Å^{-1}. In Figure 6, S_q, G_q, and C_q for PAAm gels after preparation are shown as a function of ν_2^0. The curves denoted by 1, 2, and 3 represent calculation results for gels prepared at $X = 1/61.5$, 1/66, and 1/100, respectively. Note that S_q and C_q are proportional to $R_{gel,q}$ and $R_{ex,q}$, respectively. It is seen that, in accord with the experimental results given in Figure 3, both S_q and C_q first increase

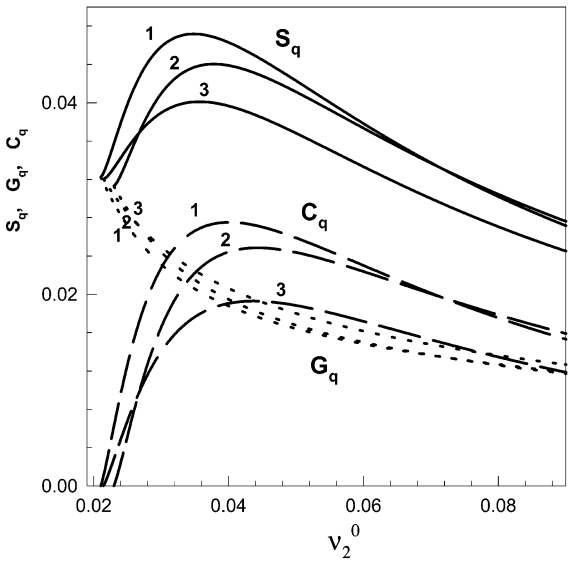

Figure 6. Variation of the theoretical structure factor S_q at $q = 0.001$ Å^{-1} for PAAm gels after preparation with the polymer network concentration ν_2^0. The contributions from thermal fluctuations G_q and from static density inhomogeneities C_q are shown by dotted and dashed curves, respectively. Calculations were using the PR theory and using the elasticity data of hydrogels prepared at a cross-linker ratio $X = 1/61.5$ (curves 1), 1/66 (curves 2), and 1/100 (curves 3).

with increasing ν_2^0, reaching a maximum at critical ν_2^0 values, and then they decrease continuously with a further increase in ν_2^0. In Figure 7A, the ratio C_q/S_q representing the contribution of the gel inhomogeneities to the scattering light intensity is plotted against ν_2^0 for each set of gels. For comparison, the experimental $R_{ex,q}/R_{gel,q}$ data are shown in Figure 7B as symbols. The curves in Figure 7B were drawn for the eye. Comparison of the experimental data with the theoretical curves shows that, although no adjustable parameter was used in the theoretical calculations, the PR theory and the experimental data share some common features. For example, the theory in conjunction with the elasticity data predicts a critical polymer concentration $\nu_{2,cr}^0$ where the degree of the inhomogeneity in PAAm gels attains a maximum value. The theory also shows that S_q, C_q, and C_q/S_q at $\nu_{2,cr}^0$ shift toward higher values as the cross-link density of gels is increased. However, clear differences between the predictions of the PR theory and the experimental behavior can also be seen from the figures. According to Figures 6 and 7A, C_q becomes maximum at $\nu_{2,cr}^0 = 0.040$, 0.044, and 0.044, while the maximum in C_q/S_q appears at $\nu_{2,cr}^0 = 0.052$, 0.060, and 0.057, for the cross-linker ratio $X = 1/61.5$, 1/66, and 1/100, respectively. However, the experimental value of $\nu_{2,cr}^0$ slightly shifts toward lower polymer concentration from 0.062 to 0.051 as the cross-linker ratio X is decreased (Figure 3). Thus, the experimental data show a decrease in $\nu_{2,cr}^0$ with decreasing cross-linker ratio X while the theory predicts that $\nu_{2,cr}^0$ is a constant or slightly shifts to higher values as X is decreased from 1/61.5 to 1/100. Furthermore, the contribution of the gel inhomogeneities to the scattering light intensity at $\nu_{2,cr}^0$ ($R_{ex,q}/R_{gel,q}$) increases from 0.8 to 1.0 with increasing cross-linker ratio, while the theory predicts an increase of the C_q/S_q ratio from 0.52 to 0.61 (Figure 7). Another point is that the theoretical curves calculated for different cross-linker ratios cross each other while the experimental curves do not show this behavior (Figure 7). These differences observed between the theory and experiments are probably due to the assumptions of the PR theory, which are unrealistic for gels formed by the free-radical mechanism.

The underlying physical picture leading to the observed phenomenon is two opposite effects of ν_2^0 on the extent of the gel inhomogeneities. As ν_2^0 is increased, the effective cross-link density ν_e of the hydrogels increases (Figure 1B), so that the spatial inhomogeneity becomes larger, resulting in an increase in $C(q)$ or $R_{ex}(q)$. Opposing this, increase in ν_2^0, i.e., increasing polymer network concentration reduces progressively the concentration difference between densely and loosely cross-linked regions of the gel, so that the apparent gel inhomogeneity decreases. The ν_2^0 dependence of $R_{ex}(q)$ is determined by a competition of these two effects. At $\nu_2^0 < \nu_{2,cr}^0$, the first effect (cross-link density) is more dominant than the second effect (concentration) so that $R_{ex}(q)$ increases with ν_2^0. At higher values of ν_2^0, the concentration effect dominates over the cross-link den-

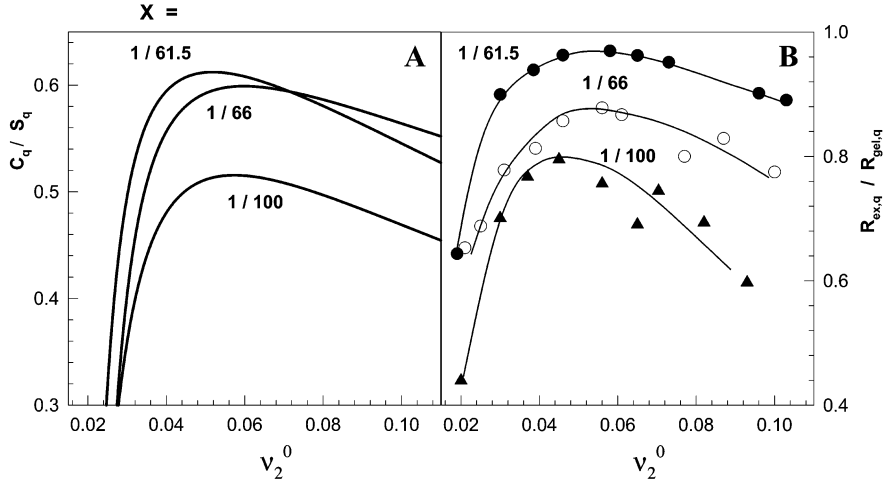

Figure 7. **(**A**)** Ratio C_q/S_q representing the contribution of the gel inhomogeneities to the scattering light intensity at $q = 0.001$ Å^{-1} shown as a function of ν_2^0. Calculations were using the PR theory and using the elasticity data of hydrogels prepared at the cross-linker ratios X indicated in the Figure. **(**B**)** Experimental $R_{ex,q}/R_{gel,q}$ data are shown as a function of ν_2^0. $X = 1/61.5$ (●), 1/66 (○), and 1/100 (▲). The curves show the trend of data.

sity effect, resulting in a continuous decrease in the excess scattering. Thus, the interplay of these two opposite effects determines the inhomogeneity in gels at the state of their preparation and results in the appearance of a maximum gel inhomogeneity at a critical initial monomer concentration.

Conclusions

The spatial inhomogeneity in PAAm gels prepared at various initial monomer concentrations was studied with the static light scattering technique. A critical polymer network concentration was found where the degree of inhomogeneity in gels attains a maximum value. This phenomenon was explained as a result of two opposite effects of the initial monomer concentration on the gel inhomogeneity. Increasing monomer concentration increases both the effective cross-link density and the polymer concentration of the hydrogels. While the inhomogeneity becomes larger due to the first effect, the latter effect decreases the apparent gel inhomogeneity. The interplay of these two opposite effects determines the spatial inhomogeneity in PAAm gels. Taking into account the ν_2^0 dependence of the effective cross-link density of hydrogels, the theory proposed by Panyukov and Rabin also predicts a maximum degree of gel inhomogeneity at a critical polymer network concentration.

Acknowledgment. We are grateful to W. Oppermann for valuable discussions and to Alexander von Humboldt Stiftung for a grant to O. Okay. This work was supported by the State Planning Organization (DPT).

References and Notes

(1) Funke, W.; Okay, O.; Joos-Muller, B. *Adv. Polym. Sci.* **1998**, *136*, 139.
(2) Okay, O. *Prog. Polym. Sci.* **2000**, *25*, 711.
(3) Shibayama, M. *Macromol. Chem. Phys.* **1998**, *199*, 1.
(4) Bastide, J.; Candau, S. J. In *Physical Properties of Polymeric Gels*; Cohen Addad, J. P., Ed.; Wiley: New York, 1996; p 143.
(5) Mallam, S.; Horkay, F.; Hecht, A. M.; Geissler, E. *Macromolecules* **1989**, *22*, 3356.
(6) Ikkai, F.; Shibayama, M. *Phys. Rev. E* **1997**, *56*, R51.
(7) Cohen, Y.; Ramon, O.; Kopelman, I. J.; Mizraki, S. *J. Polym. Sci., Polym. Phys. Ed.* **1992**, *30*, 1055.
(8) Schosseler, F.; Skouri, R.; Munch, J. P.; Candau, S. J. *J. Phys. II* **1994**, *4*, 1221.
(9) Shibayama, M.; Tanaka, T.; Han, C. C. *J. Chem. Phys.* **1992**, *97*, 6842.
(10) Horkay, F.; McKenna, G. B.; Deschamps, P.; Geissler, E. *Macromolecules* **2000**, *33*, 5215.
(11) Shibayama, M.; Ikkai, F.; Nomura, S. *Macromolecules* **1994**, *27*, 6383.
(12) Shibayama, M.; Ikkai, F.; Shiwa, Y.; Rabin, Y. *J. Chem. Phys.* **1997**, *107*, 5227.
(13) Ikkai, F.; Iritani, O.; Shibayama, M.; Han, C. C. *Macromolecules* **1998**, *31*, 8526.
(14) Hecht, A. M.; Duplessix, R.; Geissler, E. *Macromolecules* **1985**, *18*, 2167.
(15) Lindemann, B.; Schröder, U. P.; Oppermann, W. *Macromolecules* **1997**, *30*, 4073.
(16) Moussaid, A.; Candau, S. J.; Joosten, J. G. H. *Macromolecules* **1994**, *27*, 2102.
(17) Bastide, J.; Mendes, E., Jr. *Makromol. Chem. Macromol. Symp.* **1990**, *40*, 81.
(18) Takata, S.; Norisuye, T.; Shibayama, M. *Macromolecules* **2002**, *35*, 4779.
(19) Baker, J. P.; Hong, L. H.; Blanch, H. W.; Prausnitz, J. M. *Macromolecules* **1994**, *27*, 1449.
(20) Okay, O.; Kurz, M.; Lutz, K.; Funke, W. *Macromolecules* **1995**, *28*, 2728.
(21) Gundogan, N.; Melekaslan, D.; Okay, O. *Macromolecules* **2002**, *35*, 5616.
(22) Durmaz, S.; Okay, O. *Polymer* **2000**, *41*, 3693.
(23) Sayıl, C.; Okay, O. *Polymer* **2001**, *42*, 7639.
(24) Flory, P. J. *Principles of Polymer Chemistry*; Cornell University Press: Ithaca, NY, 1953.
(25) Treloar, L. R. G. *The Physics of Rubber Elasticity*; University Press: Oxford, 1975.
(26) Debye, P. J. *J. Chem. Phys.* **1959**, *31*, 680.
(27) Bueche, F. *J. Colloid Interface* **1970**, *33*, 61.
(28) Debye, P.; Bueche, A. M. *J. Appl. Phys.* **1949**, *20*, 518.
(29) Soni, V. K.; Stein, R. S. *Macromolecules* **1990**, *23*, 5257.
(30) Horkay, F.; Hecht, A. M.; Geissler, E. *Macromolecules* **1994**, *27*, 1795.
(31) Shibayama, M.; Tanaka, T. *J. Chem. Phys.* **1992**, *97*, 6829.
(32) Wu, W.; Shibayama, M.; Roy, S.; Kurokawa, H.; Coyne, L. D.; Nomura, S.; Stein, R. S. *Macromolecules* **1990**, *23*, 2245.
(33) Higgins, J. S.; Benoit, H. C. *Polymers and Neutron Scattering*; Clarendon Press: Oxford, 1994.
(34) Baumgaertner, A.; Picot, C. E. *Molecular Basis of Polymer Networks*; Springer-Verlag: Berlin, 1989.
(35) Panyukov, S.; Rabin, Y. *Macromolecules* **1996**, *29*, 7960.
(36) Hooper, H. H.; Baker, J. P.; Blanch, H. W.; Prausnitz, J. M. *Macromolecules* **1994**, *23*, 1096.

MA021366U